CAT activity was measured with a diffusion assay as previously reported (*30*).
17. M. O. Westendorp *et al*., *Nature* **375**, 497 (1995).
18. E. Serfling, A. Avots, M. Neumann, *Biochim. Biophys. Acta* **1263**, 181 (1995).
19. A. S. Wechsler, M. C. Gordon, U. Dendorfer, K. P. Le Clair, *J. Immunol.* **153**, 2515 (1994).
20. 25. P. Ghosh, T. H. Tan, N. R. Rice, A. Sica, H. A. Young, *Proc. Natl. Acad. Sci. U.S.A.* **90**, 1696 (1993).
21. G. Nabel and D. Baltimore, *Nature* **326**, 711 (1987).
22. M. Ott and E. Verdin, unpublished observation.
23. PBLs were infected with HIV infectious stocks generated after transfection of molecular clone $HIV_{89.6}$ or a mutant containing a stop codon at amino acid 72 of Tat (5×10^4 pg of p24 antigen per 10^7 cells). Culture supernatants from cells stimulated with antibodies directed against either CD3 or CD3+CD28 were harvested at different times after infection and analyzed for RT activity.
24. C. Graziosi *et al.*, *Science* **265**, 248 (1994).
25. C. Graziosi *et al.*, *Proc. Natl. Acad. Sci. U.S.A.* **93**, 4386 (1996).
26. A. L. Kinter, G. Poli, L. Fox, E. Hardy, A. S. Fauci, *J. Immunol.* **154**, 2448 (1995).
27. J. D. Fraser, B. A. Irving, G. R. Crabtree, A. Weiss, *Science* **251**, 313 (1991).
28. O. K. Haffar *et al.*, *Proc. Natl. Acad. Sci. U.S.A.* **90**, 11094 (1993).
29. S. K. Arya, C. Guo, S. F. Josephs, F. Wong-Staal, *Science* **229**, 69 (1985).
30. C. Van Lint, S. Emiliani, M. Ott, E. Verdin, *EMBO J.* **15**, 1112 (1996).
31. F. Pages *et al.*, *Nature* **369**, 327 (1994).
32. M. Adams *et al.*, *Proc. Natl. Acad. Sci. U.S.A.* **91**, 3862 (1994).
33. Anti-CD3 (454.3.21) was provided by N. Chiorazzi (North Shore University Hospital, Manhasset, NY) and precoated on tissue culture wells with 3 μg of antibody per milliliter of buffer [35 mM bicarbonate and 15 mM carbonate (pH 9.6)] at 4°C overnight. Anti-CD28 (clone 28.2) was provided by D. Olive (INSERM, Marseilles, France) (*31*).
34. To express the different forms of Tat in *Escherichia coli*, Bam HI–Bam HI fragments corresponding to either Tat72 or Tat101 cDNAs (*12*) were cloned into the unique Bam HI site of pTrcHisB behind the Trc promoter (Invitrogen). *E. coli* (TOP10 strain, Invitrogen) containing the recombinant plasmids were induced for 16 hours with isopropyl-β-D-thiogalactopyranoside (1 mM) at 37°C. Pelleted cells were resuspended in buffer A [6M guanidine hydrochloride, 0.1M NaH_2PO_4, and 0.01M tris (pH 8.0)] at 5 ml per gram wet weight and stirred for 1 hour at room temperature. Lysate was centrifuged at 10,000 rpm for 15 min at 4°C and the supernatant was collected. Four milliliters of a 50% slurry of Ni–nitrilotriacetic acid resin (Invitrogen) equilibrated in buffer A was added to the cell suspension and incubated at room temperature for 1 hour. This mixture was loaded on a column and the flowthrough was collected. The resin was washed sequentially with 10 ml of buffer A, 15 ml of buffer B [8 M urea, 0.1M NaH_2PO_4, and 0.01 M tris (pH 8.0)], and 15 ml of buffer C (same composition as buffer B, but at a pH of 6.3). The recombinant protein was eluted with 15 ml of buffer C containing 250 mM imidazole. This eluate was loaded directly on a high-performance liquid chromatography C4 column run in a gradient of acetonitrile (0 to 100%) in 0.1% trifluoroacetic acid. Fractions containing Tat were lyophilized in small aliquots and stored at –70°C under anaerobic conditions to prevent Tat oxidation. Tat was resuspended in degassed phosphate-buffered saline plus 0.1 mM dithiothreitol immediately before use. The biological activity of Tat purified according to this protocol was tested by incubating it with U1 cells, which contain a virus exhibiting a Tat-defective phenotype (*32*). Tat treatment of these cells caused a 50-fold induction of viral expression as detected by p24 secretion into culture supernatant. Endotoxin contamination of Tat prepared with this protocol was below the detection limit of the assay (<59 EU/ml; Limulus Amebocyte Lysate Assay, Biowhittaker, Walkersville, MD).
35. D. A. Mann and A. D. Frankel, *EMBO J.* **10**, 1733 (1991).
36. pIL-2luc was constructed by cloning a 390–base pair Kpn I–Hind III fragment containing the human IL-2 promoter (nt –340 to nt +50) (a gift from R. Gaynor) into the corresponding sites of pGL2-BASIC (Promega, Madison, WI). This plasmid was used as a substrate for the mutagenesis of the CD28RE by means of the Transformer site-directed mutagenesis method (Clontech, Palo Alto, CA). The oligonucleotide (5′-GGGTTTAAAGAA**GCCT**CAAAGAGTCAT-CA-3′) was used to introduce four mutations within the CD28RE (mutations are highlighted in bold), abolishing binding of the CD28RC to the element (*27*). The oligonucleotide (5′-CTTATCATGTCT**GA-CGTC**GTCGACCGATGC-3′) changes a Bam HI into an Aat II restriction site (highlighted in bold) and was used for selection during mutagenesis. The region corresponding to the IL-2 promoter was fully resequenced to confirm the mutation, and the resequenced fragment was subcloned into pGL2-BASIC as described above.
37. C. Van Lint, J. Ghysdael, P. Paras Jr., A. Burny, E. Verdin, *J. Virol.* **68**, 2632 (1994).
38. L. Osborn, S. Kunkel, G. Nabel, *Proc. Natl. Acad. Sci. U.S.A.* **86**, 2336 (1989).
39. A point mutation (C → T) was introduced into a molecular clone of $HIV_{89.6}$, p89.6 (*5*) to change codon 72 of the Tat ORF from CAG into TAG. The mutation was introduced with the use of the Transformer kit (Clontech) with the following two oligonucleotides: 5′-CTCTATCAAAGTAGTAAGTAGTAC-3′ (Tat mutation) and 5′-GTGCCACCTGATATCTA-AGAAACC-3′ (selection primer). The presence of the mutation was verified by sequencing, and a fully resequenced Sal I–Stu 1 fragment containing the mutation was subcloned back into p89.6. Supernatants from CEM × 174 cells transfected with this DNA were harvested and their RT titer was measured. To confirm that virus stocks had not reverted to wild type, virus stocks were centrifuged and purified RNA was used in RT-PCR to amplify a fragment containing the mutated Tat gene. This PCR fragment was cloned with the TA cloning kit (Invitrogen), 10 individual clones were resequenced, and all contained the original mutation in the Tat gene.
40. This paper is dedicated to the memory of Kenneth Warren. We thank R. Colmann, D. Olive, N. Chiorazzi, R. Gaynor, C. Metz, and U. Siebenlist for reagents used in these studies; L. Bonetta and K. Manogue for their helpful comments on the manuscript; D. Olive and Y. Colette for helpful discussions; K.-T. Jeang for pointing out to us the Tat mutation resulting in a truncated Tat protein; and N. Yarlett for testing cell lines for *Mycoplasma*. C.V.L. is Chargé de Recherches of the Fond National de la Recherche Scientifique, Belgium.

13 September 1996; accepted 15 January 1997

A Plastid of Probable Green Algal Origin in Apicomplexan Parasites

Sabine Köhler,*† Charles F. Delwiche,*‡ Paul W. Denny, Lewis G. Tilney, Paul Webster, R. J. M. Wilson, Jeffrey D. Palmer, David S. Roos§

Protozoan parasites of the phylum Apicomplexa contain three genetic elements: the nuclear and mitochondrial genomes characteristic of virtually all eukaryotic cells and a 35-kilobase circular extrachromosomal DNA. In situ hybridization techniques were used to localize the 35-kilobase DNA of *Toxoplasma gondii* to a discrete organelle surrounded by four membranes. Phylogenetic analysis of the *tufA* gene encoded by the 35-kilobase genomes of coccidians *T. gondii* and *Eimeria tenella* and the malaria parasite *Plasmodium falciparum* grouped this organellar genome with cyanobacteria and plastids, showing consistent clustering with green algal plastids. Taken together, these observations indicate that the Apicomplexa acquired a plastid by secondary endosymbiosis, probably from a green alga.

Apicomplexan parasites contain two maternally inherited extrachromosomal DNA elements (*1*). The mitochondrial genome is a multicopy element of ~6 to 7 kb encoding three proteins of the respiratory chain and extensively fragmented ribosomal RNAs (*2*). In addition, these parasites contain a 35-kb circular DNA molecule with no significant similarity to known mitochondrial genomes. The 35-kb element is similar to chloroplast genomes, containing an inverted repeat of ribosomal RNA genes and genes typically found in chloroplasts but not mitochondria (*rpoB*/C, *tufA*, and *clpC*) (*3*). The 35-kb DNA is also predicted to encode a complete set of tRNAs, numerous ribosomal proteins, and several unidentified open reading frames (*3*).

We used in situ hybridization to determine whether the 35-kb DNA is found within the parasite nucleus, mitochondrion, or cytoplasm or, alternatively, whether this

S. Köhler, L. G. Tilney, D. S. Roos, Department of Biology, University of Pennsylvania, Philadelphia, PA 19104, USA.
C. F. Delwiche and J. D. Palmer, Department of Biology, Indiana University, Bloomington, IN 47405, USA.
P. W. Denny and R. J. M. Wilson, National Institute for Medical Research, Mill Hill, London NW7 1AA UK.
P. Webster, Department of Cell Biology, Yale University School of Medicine, New Haven, CT 06520, USA.

*These authors contributed equally to this work.
†Present address: School of Pharmacy, University of California, San Francisco, CA 94143, USA.
‡Present address: Department of Plant Biology, University of Maryland, College Park, MD 20742, USA.
§To whom correspondence should be addressed. E-mail: droos@sas.upenn.edu

molecule localizes to a previously unidentified DNA-containing organelle. We chose *T. gondii* for this project (rather than *Plasmodium*, in which the 35-kb element has been better characterized) for two reasons. First, there are approximately eight copies of the 35-kb circle per haploid genome in *T. gondii* tachyzoites, as opposed to approximately one copy in *Plasmodium*. Second, *Toxoplasma* offers much better ultrastructural resolution, because of its regular organization of intracellular organelles and well-defined apical region. To localize the 35-kb DNA, we hybridized extracellular tachyzoites with digoxigenin-labeled DNA probes that covered 10.5 kb of the 35-kb genomic sequence but excluded the ribosomal genes, to avoid cross-hybridization with the mitochondrial genome (*4*). We also targeted RNA transcripts derived from the 35-kb genome, using digoxigenin-labeled antisense RNA generated from putative *rps4* sequences (*5*). The DNA:DNA or RNA:RNA hybrids were visualized by fluorescence in situ hybridization (FISH), and nuclear DNA was counterstained with the fluorescent dye YOYO-1. Examination by laser-scanning confocal microscopy revealed that the 35-kb DNA of *T. gondii* is localized to a specific region in the cell, adjacent to (but distinct from) the apical end of the parasite nucleus (Fig. 1A). Transcripts of *rps4* were also concentrated in this region (Fig. 1B), suggesting that diffusion of 35-kb DNA-related transcripts is restricted by a physical (possibly membranous) barrier.

Extranuclear DNA was not detected by YOYO-1 (or propidium iodide), presumably because of the low DNA concentrations typically found in non-nuclear organelles and the membrane-impermeable nature of these dyes. However, the extranuclear signal obtained by FISH resembled the pattern observed after staining with sensitive membrane-permeable DNA dyes such as Hoechst 33258 or 4′,6′-diamidino-2-phenylindole (DAPI) (Fig. 1, D and E). To compare the subcellular distribution of extranuclear DNA with the 35-kb DNA-derived FISH signal (Fig. 1, F though H), we used a monoclonal antibody to DNA because neither Hoechst nor DAPI stains are excited by the Kr-Ar laser that was available for confocal imaging and because in situ signals were difficult to detect on a conventional fluorescence microscope.

To examine the subcellular location of the 35-kb DNA more precisely, we hybridized frozen ultrathin sections with digoxigenin-labeled DNA probes (Fig. 2, A and B). Staining with antidigoxigenin followed by a secondary antibody and gold-conjugated protein A localized the 35-kb element to a membranous region adjacent to the nucleus but distinct from either the mitochondrion or the Golgi apparatus (large gold particles). Antibody to DNA also stained this area (small gold particles). In control experiments, probes prepared from plasmid vector DNA showed no hybridization, although the antibody to DNA still detected the membranous region just apical to the nucleus. The morphology of the membranous structure labeled by 35-kb DNA probes is difficult to resolve under the harsh conditions used for in situ hybridization, but conditions suitable for labeling with antibody against DNA alone revealed an organelle associated with multiple membranes (Fig. 2C). Thin sections through Epon-embedded parasites (which provide superior membrane preservation but do not permit antibody or in situ labeling) show that this organelle is invariably enclosed by four bilayer membranes (Fig. 2, D and E).

Previous phylogenetic studies on the 35-kb genome suggested a plastid ancestry, but confidence in this assessment has been low because of the limited number of taxa and phylogenetic methods used (*6*). Genes identified on the 35-kb element include *tufA*, encoding the protein synthesis elongation factor Tu, a gene previously found useful for constructing molecular phylogenies (*7*). Phylogenetic analysis of *tufA* sequences from *T. gondii*, *P. falciparum*, and *E. tenella* (*8*) places the apicomplexan 35-kb element solidly within the plastids (Fig. 3). This placement is robust when either amino acid alignments or nucleotide alignments first and second codon positions are analyzed under a variety of phylogenetic methods, including maximum likelihood, parsimony, and distance methods (using either Kimura three-parameter or LogDet transformation) (*9*). The association of apicomplexan *tufA* genes with those of plastids does not appear to be caused by either the AT-rich or the divergent nature of the sequences (*10*). The similarity of apicomplexan and plastid *tufA* genes is also supported by the presence of two insertions characteristic of plastids and cyanobacteria, although the length of these insertions is variable among the Apicomplexa.

All three phylogenetic methods used sup-

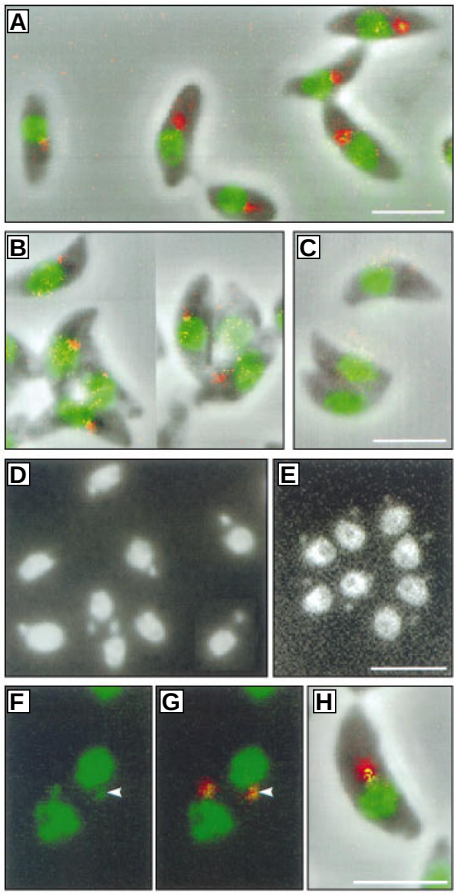

Fig. 1. The 35-kb episomal genome and 35-kb derived RNA transcripts localize to a specific region adjacent to the nucleus in *T. gondii* tachyzoites. (**A**) Pseudocolor image of *T. gondii* tachyzoites hybridized with digoxigenin-labeled 35-kb genome-specific DNA (*26*). The DNA:DNA hybrids were visualized with rhodamine-conjugated anti-digoxigenin (red), and nuclear DNA was counterstained with YOYO-1 (green). Signals derived from the two fluorophores were collected independently by laser scanning confocal microscopy and merged with phase-contrast images simultaneously collected from the transmitted-light flow-through from the confocal microscope. (**B** and **C**) Localization of 35-kb DNA-encoded *rps4* transcripts (*27*). Tachyzoites were hybridized with digoxigenin-labeled (B) antisense or (C) sense RNA generated in vitro from a cloned DNA fragment spanning the putative *rps4* gene and visualized with rhodamine as above (red); nuclei were counterstained with YOYO-1 (green). (**D** and **E**) Extrachromosomal DNA in *T. gondii* tachyzoites. Fixed parasites were stained for 20 min at 25°C with ~2 μg/ml of Hoechst 33258 in 1× SSC and examined by conventional epifluorescence microscopy with a Zeiss Axiovert 35 equipped with an ultraviolet filter set. A distinct extranuclear signal is seen in extracellular tachyzoites (D). Intracellular tachyzoites (E) orient in "rosettes," with their apical ends pointed outward (*28*), permitting localization of the extranuclear DNA to the apical juxtanuclear region. (**F** through **H**) Co-localization of extranuclear DNA and 35-kb genome-specific sequences. Nuclei were labeled with YOYO-1 and extranuclear DNA with an antibody directed against DNA, followed by a fluorescein-conjugated secondary antibody (green). (Nuclear DNA was not labeled by the antibody to DNA except under extraction conditions, that destroyed parasite morphology, presumably because binding is blocked by chromatin-associated proteins.) The extranuclear DNA co-localizes with in situ hybridization probes derived from the 35-kb element (red). (F and G) Green and green + red images of the same field (containing two parasites); (H) green and red fluorescence signals from a different parasite, merged with the corresponding phase-contrast image. Scale bars, 5 μm.

port monophyly of all plastids, including the apicomplexan 35-kb element. Resampling methods that test the internal consistency of phylogenetic patterns within the data gave bootstrap values (*11*) of 75, 39, and 88% for monophyly of plastids (for maximum likelihood, LogDet–neighbor-joining, and parsimony analyses, respectively) and 81, 69, and 94% for monophyly of plastids and cyanobacteria (Fig. 3). Parsimony analysis of nucleotide data scored only for transversion events also provides strong support for the clade composed of cyanobacteria and plastids (94%), and moderate support (78%) for plastid monophyly. The apicomplexan plastids were consistently placed among the green algae by all analytical methods used. Although support for green algal affinity was weak (bootstrap values of 41, 21, and 63%), these values are comparable to the level of support for green plastid monophyly when apicomplexans are excluded, yet the green plastids are known to be monophyletic on many other grounds (*7*). Trees constrained to place the Apicomplexa with non-green plastids were consistently worse than those placing them with the green plastids, although the difference in likelihood was not significant by the Kishino-Hasegawa test (*9*).

Many investigators have assumed that the apicomplexan 35-kb genome is related to dinoflagellate plastids, on the basis of structural similarities between the Apicomplexa and dinoflagellates, and phylogenetic analyses of nuclear genes (*12*). Unfortunately, few dinoflagellate plastid genes have been examined, but there is considerable diversity of plastid form among dinoflagellates, and their plastids may have arisen from multiple distinct endosymbioses (*13*). Thus, it seems likely that the last common ancestor of all dinoflagellates was not photosynthetic and that the Apicomplexa and dinoflagellates acquired their plastids independently.

A structure consisting of multiple membranes has previously been described as the "Golgi adjunct" in *Toxoplasma*, and similar structures—variously termed the lamellärer körper, vacuoles plurimembranaires, spherical body, or Hohlzylinder—have been observed in other apicomplexan parasites (*14*). The cytological derivation of this structure has been unclear, but the demonstration that this organelle is associated with a plastid genome in *Toxoplasma*—combined with the monophyly of *Toxoplasma*, *Plasmodium*, and *Eimeria tufA*s in all analyses—argues for a single endosymbiotic organelle common to all apicomplexans. The apicomplexan plastid (abbreviated "apicoplast") is an authentic plastid in all respects, albeit one that is probably incapable of photosynthesis.

Previous investigators have debated the number of membranes surrounding the apicoplast, suggesting that the appearance of multiple membranes may result from proximity to

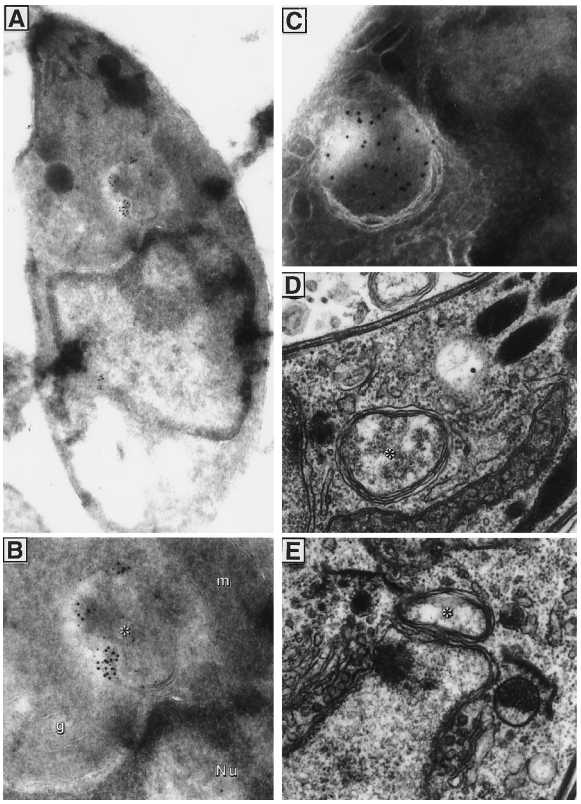

Fig. 2. Ultrastructural localization of 35-kb genome-specific DNA to a unique organelle enclosed by four membranes in *T. gondii* tachyzoites. (**A**) Longitudinal ultrathin cryosection of *T. gondii* tachyzoites hybridized with digoxigenin-labeled probes derived from the 35-kb DNA (*29*). Digoxigenin was visualized with antibodies and protein A coupled to 10-nm gold particles. Samples were further incubated with monoclonal antibody directed against DNA (which does not stain intact chromatin in the parasite nucleus; see Fig. 1 legend), followed by a secondary antibody with protein A coupled to 5-nm gold (*30*). (**B**) Higher magnification of the region in (A) showing gold labeling. The 35-kb DNA probes hybridize specifically with a membranous region (*) just apical to the nucleus (Nu) but are distinct from the mitochondrion (m) and Golgi apparatus (g). (**C**) Immunogold labeling of extranuclear DNA (10-nm gold particles) in a *T. gondii* tachyzoite not subjected to in situ hybridization conditions. Membranes appear white in this negatively stained image. (**D** and **E**) Ultrathin sections through the apicoplast (*) of an Epon-embedded parasite (*31*). The organelle is surrounded by four membranes (stained black by uranyl acetate). The parasite in (E) is beginning to divide, as indicated by division of the Golgi and development of the two daughter "buds." The apicoplast is flattened adjacent to the apical end of the nucleus and is divided between the two daughters early during endodyogeny.

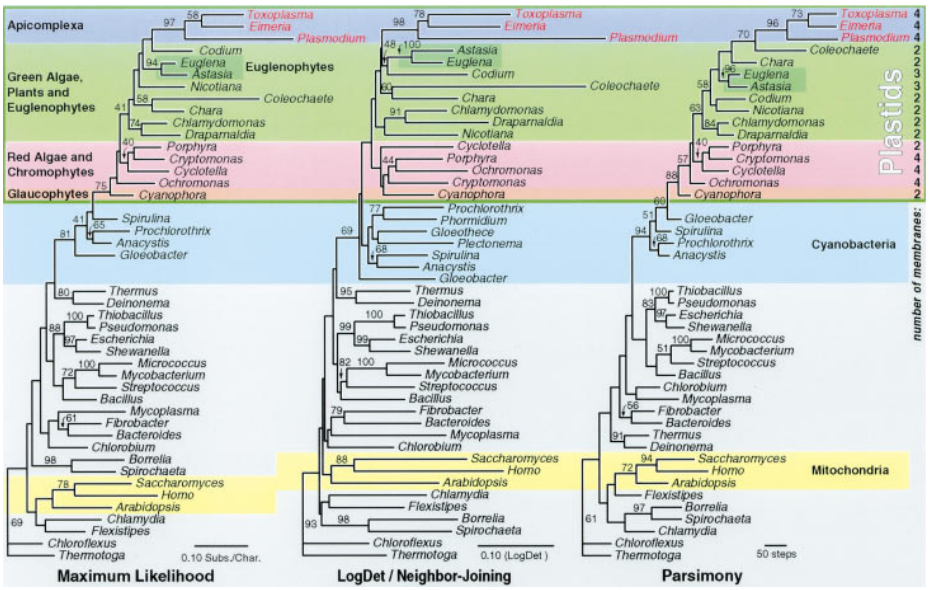

Fig. 3. Molecular phylogenetic analyses of *tufA* genes from three apicomplexan 35-kb genomes and representative eubacteria, plastids, and mitochondria (*32*). Maximum likelihood finds the phylogeny that is statistically most likely to have given rise to the observed sequences. Neighbor joining is a cluster method, in this case using "LogDet" distances (−ln determinant). Parsimony finds the tree that requires the fewest inferred mutations to represent the data (*9*). Branch lengths are proportional to the number of inferred substitutions (or LogDet value); bootstrap values ≥40% are given above the corresponding branch (*11*). The column at the far right indicates the number of membranes surrounding the plastid for taxa in the parsimony tree. All three phylogenetic methods consistently group the apicomplexan 35-kb encoded *tufA* genes with green algal plastids.

the endoplasmic reticulum or Golgi apparatus (*14*, *15*). Although this organelle is closely associated with the Golgi, the fixation and staining conditions used for Fig. 2, D and E, commonly show four membranes. It is difficult to visualize distinct membranes all the way around the organelle (and serial sections necessarily lose definition at the top and bottom of the stack), but all of our micrographs are consistent with the four-membrane hypothesis, and many sections are clearly incompatible with ≤3 or ≥5 membranes. The presence of four membranes enclosing the apicoplast suggests that it originated as a secondary endosymbiont (derived by ingestion of a eukaryote that itself harbored a plastid), analogous to the plastids of chlorarachniophytes and cryptomonads (*16*). This hypothesis is bolstered by the phylogenetic grouping of apicoplasts with green algal plastids, which presents a clear conflict with nuclear gene phylogenies (*12*, *17*) and therefore provides prima facie support for a secondary endosymbiotic origin. The putative green algal origin of apicomplexan plastids should be testable through further phylogenetic analyses of plastid sequences and analysis of apicomplexan nuclear genes of potential green algal origin, such as phosphoglucose isomerase and enolase (*18*).

The function of the apicoplast remains unknown, but the parasite faithfully replicates this organelle, which divides by binary fission and is introduced into developing daughter parasites very early during replication (Fig. 2E). The apicoplast genome is certainly transcribed: Several transcripts have been identified by Northern (RNA) blot analysis (*3*, *19*), *rps4* transcripts localize to the same region as the 35-kb DNA (Fig. 1), and ribosomal RNA derived from the 35-kb circle has been localized to this organelle (*15*). Like other endosymbiotic genomes (*20*), the 35-kb element is presumed to be the remnant of a much larger precursor, most of whose original functions have been lost or transferred to the nuclear genome. Photosynthesis is the most familiar function of plastids, and evidence for a chlorophyll binding protein in Apicomplexa has been reported (*21*), although we have not been able to confirm these results in *Toxoplasma*. Plastids also play many other key metabolic roles—including biosynthesis of amino acids and fatty acids, assimilation of nitrate and sulfate, and starch storage (*22*)—and have been maintained in many nonphotosynthetic taxa over millions of years (*23*). The apicoplast has been suggested as a target for macrolide antibiotics in *Toxoplasma* (*24*) and may also be the target for rifampicin in *Plasmodium* (*25*). Further studies are likely to elucidate important aspects of plastid function and evolutionary history, in addition to identifying other parasite-specific targets for chemotherapy.

REFERENCES AND NOTES

1. R. J. M. Wilson, D. H. Williamson, P. Preiser, *Infect. Agents Dis.* **3**, 29 (1994); J. E. Feagin, *Annu. Rev. Microbiol.* **48**, 81 (1994).
2. A. B. Vaidya, R. Akella, K. Suplick, *Mol. Biochem. Parasitol.* **35**, 3614 (1989); J. T. Joseph, S. M. Aldritt, T. Unnasch, O. Puijalon, D. F. Wirth, *Mol. Cell Biol.* **9**, 3621 (1989).
3. R. J. M. Wilson *et al.*, *J. Mol. Biol.* **261**, 155 (1996).
4. J. E. Feagin, E. Werner, M. J. Gardner, D. H. Williamson, R. J. M. Wilson, *Nucleic Acids Res.* **20**, 879 (1992).
5. The complete sequence of the *T. gondii* 35-kb DNA has been deposited in GenBank, with accession number U87145. The map of this genome is virtually identical to that of *Plasmodium* (*3*).
6. C. J. Howe, *J. Theor. Biol.* **158**, 199 (1992); M. J. Gardner *et al.*, *Mol. Biochem. Parasitol.* **66**, 221 (1994).
7. B. Cousineau, C. Cerpa, J. Lefebvre, J. Cedergren, *Gene* **120**, 33 (1992); W. Ludwig *et al.*, *Antonie van Leeuwenhoek* **64**, 285 (1993); C. F. Delwiche, M. Kuhsel, J. D. Palmer, *Mol. Phylogenet. Evol.* **4**, 110 (1995); S. L. Baldauf, J. D. Palmer, W. F. Doolittle, *Proc. Natl. Acad. Sci. U.S.A.* **93**, 7749 (1996).
8. Predicted protein sequences for Apicomplexan *tufA* genes are available from GenBank; accession numbers: *T. gondii*, X88775; *P. falciparum*, X87630; and *E. tenella*, X89446.
9. D. M. Hillis, C. Moritz, B. K. Mable, Eds., *Molecular Systematics* (Sinauer, Sunderland MA, 1996).
10. The apicomplexan *tufA* genes are 70 to 80% A-T (~95% at third-codon positions), versus 48% (43%) for bacterial *tufA* genes and 66% (84%) for plastid *tufA*s. Biases in base composition can influence phylogenetic analysis [P. J. Lockhart, M. A. Steel, M. D. Hendy, D. Penny, *Mol. Biol. Evol.* **11**, 605 (1994)], but bias-tolerant methods such as transversion and LogDet analyses consistently place the 35-kb element well within the plastids. Although apicomplexan *tufA*s are highly divergent (*Plasmodium* in particular) and therefore may be vulnerable to "long branch" effects [J. Felsenstein, *Syst. Zool.* **27**, 401 (1978); D. M. Hillis, J. P. Huelsenbeck, C. W. Cunningham, *Science* **264**, 671 (1994); J. H. Kim, *Syst. Biol.* **45**, 363 (1996)], the Apicomplexa remain within the plastids even in the presence of the rapidly evolving mitochondrial and *Mycoplasma* genes. Only the association with *Coleochaete* in parsimony analyses is a probable example of long-branch effects.
11. J. Felsenstein, *Annu. Rev. Genet.* **22**, 521 (1988).
12. N. D. Levine, *J. Protozool.* **35**, 518 (1988); A. A. Gajadhar *et al.*, *Mol. Biochem. Parasitol.* **45**, 147 (1991); T. Cavalier-Smith, *Microbiol. Rev.* **57**, 953 (1993); Y. Van de Peer, S. A. Rensing, U.-G. Maier, R. De Wachter, *Proc. Natl. Acad. Sci. U.S.A.* **93**, 7732 (1996).
13. J. D. Dodge, in *The Chromophyte Algae: Problems and Perspectives*, J. C. Green, B. S. C. Leadbeater, W. L. Diver, Eds. (Clarendon, Oxford, 1989), pp. 207–227.
14. M. E. Siddall, *Parasitol. Today* **8**, 90 (1992).
15. G. I. McFadden, M. E. Reith, J. Mulholland, N. Lang-Unnasch, *Nature* **381**, 482 (1996).
16. G. I. McFadden and P. R. Gilson, *Trends Ecol. Evol.* **12**, 12 (1995).
17. S. L. Baldauf and J. D. Palmer, *Proc. Natl. Acad. Sci. U.S.A.* **90**, 11558 (1993).
18. D. Van Der Straeten, R. A. Rodrigues-Pousada, H. M. Goodman, M. Van Monagu, *Plant Cell* **3**, 719 (1991); M. Read, K. E. Hicks, P. F. G. Sims, J. E. Hyde, *Eur. J. Biochem.* **220**, 513 (1994); L. A. J. Katz, *J. Mol. Evol.* **43**, 453 (1996).
19. J. E. Feagin and M. E. Drew, *Exp. Parasitol.* **80**, 430 (1995).
20. J. D. Palmer, *Annu. Rev. Genet.* **19**, 325 (1985); M. W. Gray, *Annu. Rev. Cell Biol.* **5**, 25 (1989).
21. J. H. P. Hackstein *et al.*, *Parasitol. Res.* **81**, 207 (1995).
22. G. Hrazdina and R. R. Jensen, *Annu. Rev. Plant Physiol. Plant Mol. Biol.* **43**, 241 (1992).
23. C. W. de Pamphilis and J. D. Palmer, *Nature* **348**, 337 (1990); K. H. Wolfe, C. W. Morden, J. D. Palmer, *Proc. Natl. Acad. Sci. U.S.A.* **89**, 10648 (1992).
24. C. J. M. Beckers *et al.*, *J. Clin. Invest.* **95**, 367 (1995); M. M. Fichera, M. K. Bhopale, D. S. Roos, *Antimicrob. Agents Chemother.* **39**, 1530 (1995).
25. S. Pukrittayamee, C. Viravam, P. Charoenlarp, Y. Yeamput, R. J. M. Wilson, *Antimicrob. Agents Chemother.* **38**, 511 (1994).
26. We prepared nick-translated DNA probes covering 10.5 kb of the *T. gondii* 35-kb circle by incubating 1 to 2 μg of template DNA for 2 hours at 14°C in a 50-μl reaction mixture containing 50 mM tris (pH 7.8), 0.1 mM digoxigenin-11–deoxyuridine 5′-triphosphate (dUTP) (Boehringer-Mannheim), 0.4 mM dATP, 0.4 mM dCTP, 0.4 mM dGTP, 5 mM $MgCl_2$, 10 mM dithiothreitol, 2.5 μg of nuclease-free bovine serum albumin, 10 U of DNA Polymerase I, and DNase I at concentrations titrated to produce labeled fragments with an average length of ~150 bp. RH-strain *T. gondii* tachyzoites were cultured in vitro in primary human fibroblasts [D. S. Roos, R. G. K. Donald, N. S. Morrissette, A. L. C. Moulton, *Methods Cell Biol.* **45**, 27 (1994)], resuspended in phosphate-buffered saline (PBS) at ~5×10^7 parasites/ml, attached to silane-coated glass slides, and fixed for 10 min at 25°C in a solution of 4% formaldehyde, 65% methanol, and 25% glacial acetic acid, followed by two 5-min fixations in methanol and glacial acetic acid (3:1). Slides were rinsed twice for 5 min in 100% ethanol, rehydrated, and permeabilized for 10 min at 25°C in Proteinase K at concentrations from 0.1 to 1.0 μg/ml (optimal concentrations varied from batch to batch) in 10 mM tris (pH 8.0) containing 5 mM EDTA. Specimens were then fixed for 5 min on ice in PBS-buffered 4% formaldehyde, rinsed twice in PBS, and incubated for 5 min in 2× standard saline citrate (SSC). Intracellular RNA was removed by digestion for 1 to 2 hours in a 200-μg/ml solution of DNase-free RNase A (in 2× SSC), followed by dehydration through an ethanol series. Parasite DNA was denatured for 5 min at 70°C in 70% formamide (in 2× SSC), chilled in ice-cold 70% ethanol, and dehydrated. Hybridization was carried out for 12 hours at 37°C in a 15-μl volume [10 ng of heat-denatured probe, 1 μg of yeast tRNA, and 1 to 2 μg of heat-denatured calf thymus DNA per microliter of 50% formamide, 10 mM tris (pH 7.4), 300 mM NaCl, 1 mM EDTA (pH 8), 10% dextran sulfate, and 1× Denhardt's solution]. After hybridization, the slides were rinsed in 4× SSC and twice washed for 10 min at 25°C in 4× SSC, twice for 3 min at 37°C in 50% formamide (in 2× SSC), twice for 5 min at 37°C in 2× SSC, once for 2 min at 25°C in 2× SSC, and twice for 5 min at 25°C in 4× SSC. We visualized the hybrids by incubating the specimens for 40 min at 25°C in 4× SSC containing rhodamine-conjugated polyclonal sheep anti-digoxigenin (Boehringer) and 0.5% nuclease-free blocking reagent. Control hybridizations with labeled pGEM-3 vector DNA showed no signal. Nuclear DNA was stained for 20 min at 25°C with 2.5 nM YOYO-1 (Molecular Probes) in 1× SSC. In Fig. 1, F through H, extranuclear DNA was stained with a monoclonal antibody raised against double-stranded DNA (Boehringer), followed by a secondary fluorescein isothiocyanate (FITC)–conjugated rabbit-antimouse antibody (Pierce). Both YOYO and FITC were visualized with a fluorescein filter set. Specimens were mounted in Aqua-Poly/Mount (Polysciences) and analyzed with a Leitz scanning confocal microscope equipped with a Kr-Ar laser, FITC and tetramethyl rhodamine isothiocyanate filter sets, and a transmitted-light detector.
27. Antisense- and sense-RNA probes were prepared by standard procedures, with the use of the T7 and Sp6 promoters in pGEM-3, flanking a 0.7-kb cloned fragment from the *T. gondii* 35-kb genome predicted to encode *rps4* (*5*). Freshly harvested parasites were fixed for 5 min at 25°C in 4% PBS-buffered formaldehyde, washed in PBS, attached to silane-coated slides, fixed for 5 min on ice in 4% formaldehyde, briefly washed in PBS, and treated with Proteinase K. After another 5 min of fixation on ice in 4% formaldehyde, the slides were washed in PBS, dehydrated, and incubated with 15 μl of hybridization solution (*26*), at probe concentrations of 1 to 2 ng/μl. Nuclear DNA was counterstained with YOYO-1.

28. N. S. Morrissette, V. Bedian, P. Webster, D. S. Roos, *Exp. Parasitol.* **79**, 445 (1994).
29. Extracellular tachyzoites were fixed for 1 hour on ice in 4% PBS-buffered formaldehyde and then for 12 hours at 4°C in 8% PBS-buffered formaldehyde. The cell suspension was embedded in 10% gelatin, incubated for 2 hours at 4°C in PBS containing 2.3 M sucrose, and frozen in liquid nitrogen. Ultrathin sections of the frozen samples were freshly prepared before each hybridization experiment. Cryosections were transferred to grids and digested for 40 min at 37°C in 2× SSC containing 200 μg/ml of DNase-free RNase A. Cellular DNAs were denatured for 5 min at 70°C in 70% formamide (in 2× SSC), chilled on ice, transferred to 50% formamide (in 2× SSC), and incubated briefly at 25°C. Sections were hybridized for 12 hours at 37°C in a humidified chamber in 5 μl of hybridization mix containing 10 to 20 ng/μl of DNA probe (*26*), washed three times for 5 min at 25°C in 4× SSC, twice for 3 min at 37°C in 50% formamide (in 2× SSC), twice for 5 min at 25°C in 2× SSC, and kept in 4× SSC at 25°C before staining. Hybridized probe was detected with polyclonal sheep anti-digoxigenin, followed by a secondary rabbit antibody directed against sheep immunoglobulin G (Pierce), and Protein A conjugated to 10-nm particles of gold. Immunogold-labeled sections were blocked for 20 min at 25°C in 4× SSC containing 0.5% blocking reagent and were incubated with a monoclonal antibody against DNA, followed by a rabbit anti-mouse secondary antibody and protein A conjugated to 5-nm gold particles. To improve the contrast of membranous structures, we counterstained hybridized cryosections on ice for 10 min in 0.3% aqueous uranyl acetate plus 2% methylcellulose. Grids were air-dried on loops and examined with a Phillips EM400 microscope.
30. The antibody directed against DNA used in Fig. 2A probably recognizes both endogenous DNA and the digoxigenin-labeled probe. Similarly, the 5-nm gold–protein A conjugate used to visualize this antibody (by means of a secondary rabbit antibody) is potentially able to recognize any anti-digoxigenin that remained unblocked. Comparable staining with antibody against DNA was observed even in the absence of a DNA probe, however (Fig. 2C), or when control plasmid was used as a probe. Cryosections labeled with antibody to DNA before the application of anti-digoxigenin also showed co-localization of large and small gold particles. The apparent clustering of label in Fig. 2, A and B, may be an artifact of in situ hybridization conditions, because antibody directed against DNA labels the organelle uniformly (Fig. 2C).
31. Infected cultures were fixed for 45 min in freshly prepared 50 mM phosphate buffer (pH 6.3) containing 1% glutaraldehyde and 1% OsO_4, rinsed in distilled water, stained in 0.5% uranyl acetate overnight, dehydrated, and embedded in Epon. Ultrathin sections were picked up on uncoated grids, stained with uranyl acetate and lead citrate, and examined with a Phillips 200 electron microscope.
32. A total of 65 sequences, including nearly all available bacterial sequences and representative plastid sequences, were aligned using PILEUP [Genetics Computer Group, Madison, WI (1991)], with manual refinement on the basis of secondary structural information. Maximum likelihood analysis was performed with fastDNAml v1.0.6 [G. J. Olsen, H. Matsuda, R. Hagstrom, R. Overbeek, *CABIOS* **10**, 41 (1994)], compiled as parallel code running on an Intel Paragon 64-node partition. Three random addition sequences and global swapping were used, but it cannot be guaranteed that the tree found is the highest likelihood tree possible. Bootstrap data sets and consensus trees were generated using PHYLIP tools SEQBOOT and CONSENSE [J. Felsenstein, University of Washington, Seattle, WA (1993)]. Bootstrap replicates were analyzed with fastDNAml using a single random addition sequence and local branch swapping only. LogDet, parsimony, and constraint analyses were performed with PAUP*4.0d48 [D. L. Swofford; Smithsonian Institution, Washington, DC (1996)] using nucleotide data from the first and second codon positions, and bootstrapping was carried out using 100 replicates with random addition sequences (where appropriate). LogDet distances are not directly comparable to standard distances but yield additive distances under any Markov model when sites are evolving independently and at the same rate (*9*).
33. This work was supported by NIH grants AI-31808 (D.S.R.) and GM-52857 (L.G.T.), NSF grant DEB-93–18594 (J.D.P.), and the University of Pennsylvania Program in Computational Biology. P.W.D. was supported by a Medical Research Council studentship, and R.J.M.W. by the United Nations Development Program–World Bank–World Health Organization Special Programme for Research in Tropical Diseases. D.S.R. is a Burroughs Wellcome New Investigator in Molecular Parasitology and a Presidential Young Investigator of the NSF, with support from Merck Research Laboratories and the MacArthur Foundation. We wish to thank R. G. K. Donald for molecular clones derived from the *T. gondii* 35-kb element, L. Chicoine for assistance with cryosectioning, J. F. Dubremetz for suggesting that the apicomplexan plastid described herein be designated the apicoplast, and P. Kuhlman, F. Lutzoni, K. Pryer, and D. Williamson for helpful discussions.

16 September 1996; accepted 27 December 1996

TECHNICAL COMMENTS

Evidence for a Family of Archaeal ATPases

The analysis by Carol J. Bult *et al.* of the *Methanococcus jannaschii* genome included families of paralogous proteins that did not seem to have counterparts in the current sequence databases (*1*). The largest of such families consists of 13 chromosomal and three plasmid-encoded proteins, which were found to be highly similar to one another [figure 6 in (*1*)], but did not show statistically significant similarity to any proteins, thus escaping functional prediction. Our inspection of the alignment, however, indicates that two of the conserved sequence blocks correspond to well-characterized functional motifs: namely, the phosphate-binding P-loop and the Mg^{2+}-binding site that are conserved in a vast variety of ATPases and GTPases (Fig. 1 and *2–4*). Even though most commonly used methods for database search such as BLASTP (*5*) showed only marginally significant similarity to several ATPases, a new version of the BLASTP program that constructs local alignments with gaps (*6*) indicated a probability of matching by chance between 10^{-4} and 10^{-6} for some of the proteins in the new archaeal family and bacterial DnaA proteins; the conservation was particularly notable in the two ATPase motifs (Fig. 1). Thus, even though these 16 proteins comprise a novel family that is so far represented only in archaea, they appear to belong to a known broad class of proteins, and we predict that they possess ATPase activity.

Screening of the nonredundant protein sequence database at the National Center for Biotechnology Information (National Institutes of Health, Bethesda, MD), with a bipartite pattern representing the specific forms of the two ATPase motifs conserved in the *M. jannaschii* family—namely, hhhhGx_4-GK[TS]$x_n$hhhhD[DE] (h indicates a bulky hydrophobic residue), selected 271 proteins, all of which are either known to possess ATPase activity or are highly similar to ATPases. In addition to DnaA, this list includes a number of members of the so-called AAA ATPase family (*7*); the similarity between these proteins and DnaA has been noted before (*4*). Many of the AAA family proteins possess chaperone-like activity and, in particular, are involved in ATP-dependent proteolysis; examples include bacterial proteins ClpA, ClpB, ClpX, FtsH, and HslU; proteasome components; and yeast HSP78 (*7*). Members of the novel archaeal protein family could also perform chaperone-like functions. This is particularly plausible, because *M. jannaschii* does not encode several molecular chaperones that are ubiquitous and highly conserved in bacteria and eukaryotes—namely, members of the HSP70, HSP90, and HSP40 families. It remains to be seen how typical is this situation in archaea.

Finally, the family of putative ATPases contains a third strikingly conserved motif with two invariant histidines and one invariant cysteine (Fig. 1). Even though this motif did not show statistically significant similarity to any proteins in the database, this may be a specific metal-binding site, and some resemblance of the divalent cation-binding motif in bacterial Fur proteins that are metal-dependent transcription regulators (*8*) could be detected (Fig. 1). Two observations seem relevant: (i) One of the chaperone ATPases, FtsH, contains a metal-binding motif conserved in its bacterial and eukaryotic homologs and is a Zn-dependent protease (*9*). (ii) *Methanococcus jannaschii* encodes at least two other putative ATPases, namely, the predicted proteins MJ0578 and MJ0579 that also contain a metal-binding domain, in these cases a ferredoxin-like domain (*10*).

Thus, analysis of conserved motifs and application of additional methods for sequence database search yields specific functional predictions for archaeal proteins that initially appeared to comprise a unique family. There is little doubt that further exploration of the *M. jannaschii* genome sequence will bring more interesting findings.

Eugene V. Koonin, *National Center for Biotechnology Information, National Library of Medicine, National Institutes of Health, Bethesda, MD 20894, USA*

A Plastid of Probable Green Algal Origin in Apicomplexan Parasites

Sabine Köhler, Charles F. Delwiche, Paul W. Denny, Lewis G. Tilney, Paul Webster, R. J. M. Wilson, Jeffrey D. Palmer and David S. Roos

Science **275** (5305), 1485-1489.
DOI: 10.1126/science.275.5305.1485